Earthquake performance and permanent displacements of shallow foundations

J.C.W. Toh

Tonkin and Taylor Ltd.

M.J. Pender

University of Auckland.

2008 NZSEE
Conference

ABSTRACT: The standard approach to seismic design of shallow foundations is equivalent to ensuring that the bearing strength factor of safety does not fall below a certain value. However, brief instances of bearing failure (yielding) during an earthquake may not necessarily be serious. A more important consideration will be the residual foundation displacements accumulated at the end of the earthquake. Macro-elements provide a simple way of capturing the essential features of soil-foundation interaction, including the residual foundation displacements, and are readily amenable to routine structural analysis.

The shallow foundation macro-element examined in this study is based on existing macro-elements. It accounts for both the elastic (small displacement) and plastic (yielding) phases of dynamic behaviour. Modelling with the macro-element produces important insights into shallow foundation performance. Permanent vertical displacement (settlement) of the foundation is predicted to accumulate only if there are many instances during an earthquake when yielding beneath the foundation occurs, with the magnitude of residual settlement being dependent on the earthquake magnitude and duration, and the static vertical factor of safety against bearing failure. Residual rotation and translation of the foundation is inferred to be dependent on the characteristics of an individual earthquake.

1 INTRODUCTION

A long established practice in assessing the stability of slopes under earthquake loading is to use the residual displacements after the earthquake as a criterion for satisfactory or unsatisfactory performance; Newmark (1965) proposed this in his Rankine lecture. Since then it has been used extensively in slope engineering and also for assessing the earthquake performance of gravity retaining structures (Richards and Elms, 1979).

Despite these developments, the same thinking seems not to have been applied to earthquake resistant design of shallow foundations. The standard LRFD seismic design approach is to use a strength reduction factor of about 0.5 on the theoretical bearing strength, with unit factoring of the foundation actions. Reverting momentarily to old-style terminology, this is roughly equivalent to requiring that the bearing strength factor of safety must not fall below 2. One can ask: how serious would it be if the foundation experienced bearing strength failure for brief periods during the passage of an earthquake? In other words, what residual foundation displacements would have accumulated at the end of the earthquake? If the displacements are acceptable then the foundation performance would be considered satisfactory, regardless of whether or not bearing failure had occurred.

This question is addressed herein by following one particular method for modelling the response of a structure-shallow foundation system to earthquake excitation. The basic procedure is to use a macro-element to represent the way the foundation and the underlying soil interact. The macro-element

provides a single computational entity to represent all the response (elastic, bearing failure, and plastic) between the foundation and the underlying soil. Clearly, this is a substantial idealisation but it has the advantage that calculations require only modest resources and so one can gain useful insights about important aspects of structure-foundation-soil interaction. In particular, in the context of this paper, we show the insights gained into the amount of deformation that might accumulate during the passage of an earthquake.

2 MACRO-ELEMENT CONCEPT

The basic model we use consists of three parts: the superstructure (i.e. the above-ground part of the structure), a foundation block (often of larger plan dimensions than the superstructure), and the underlying soil. The superstructure is represented in this paper as a single degree of freedom structure. The foundation block, assumed to be rigid, is able to move laterally and vertically, and also to rotate.

We know that for small levels of excitation the system will respond elastically and the elastic compliance of the soil beneath the foundation will lengthen the natural period of the system beyond that of the fixed base structure. This is the basis of "classical" soil-structure interaction modelling. Secondly, for larger levels of excitation there may be nonlinear behaviour of the soil beneath the foundation following the well-known degradation of the shear modulus with increasing level of shear strain, which is accompanied with increasing material damping. Table 4.1 of Eurocode 8, Part 5, suggests an approximate way of allowing for this as the peak ground acceleration increases. Thirdly, for even higher levels of excitation, there is the possibility of bearing strength failure, resulting in plastic deformations being induced beneath the foundation. Shallow foundation bearing strength is a complex function of the vertical load on the foundation, the horizontal shear and the moment; all combinations of these three actions that lead to bearing failure generate a bearing strength surface. In addition there may be instances of a loss of contact between parts of the underside of the foundation and the underlying soil during the earthquake motion.

All possible phases of the interaction outlined above are contained in the macro-element model of foundation-soil interaction. What is attractive about the macro-element is that all aspects of elastic and plastic behaviour of the foundation block shown conceptually in Figure 1 are encompassed in one computational entity. The entire soil-foundation system is described by the behaviour of a single point at the centre of the foundation. All the essential characteristics of foundation response can be captured by the macro-element; however no detailed information about the behaviour of the soil mass or individual soil elements is available. In this way, the macro-element is primarily intended to be a design tool.

The macro-element behaviour is bounded by two well defined limits. There is first the small strain elastic vertical, lateral and rocking stiffnesses of the foundation, which control the response of the foundation at low levels of excitation. Secondly, there is the ultimate state defined by the bearing strength surface of the foundation, which limits the magnitude of the actions that the foundation can sustain. When the actions lie on the bearing strength surface plastic deformations will be induced. Much of the thinking behind the plastic part of the macro-element is borrowed from work hardening plasticity, common in finite element software for predicting stresses and strains in an element in a continuum mesh. For the macro-element, similar concepts are applied to the global response of the block of soil beneath the foundation, with the model expressed in terms of actions and displacements rather than stresses and strains.

The macro element concept was first proposed by Nova and Montrasio (1991) for static loading, and was developed for earthquake response of shallow foundations by Paolucci (1997), Cremer et al (2001), Houlsby and Cassidy (2002), Gajan et al (2005), and Chatzigogos et al (2007a). Muir Wood (2007) has also developed macro element modelling for static and dynamic retaining wall behaviour.

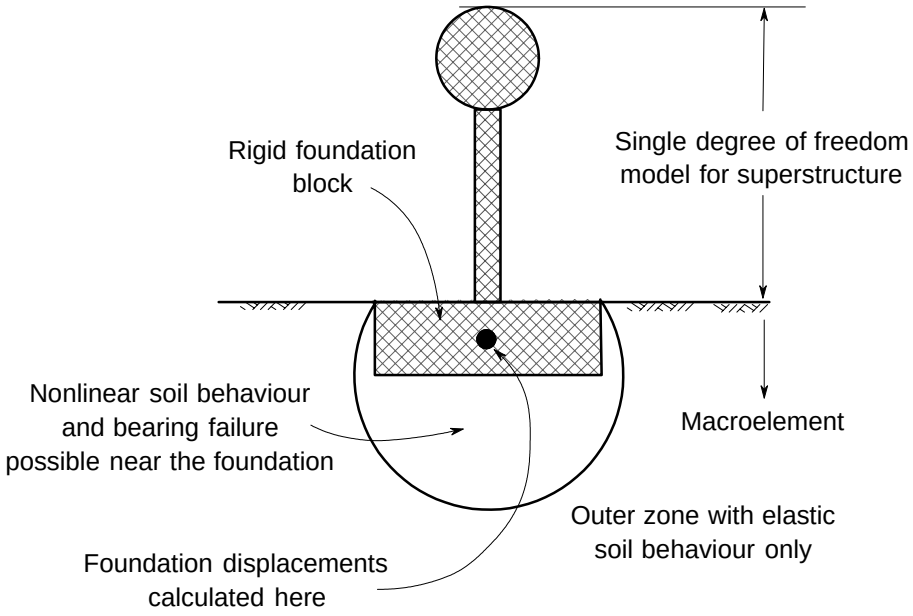

Figure 1: Macro element concept (after Chatzigogos et al, 2007a)

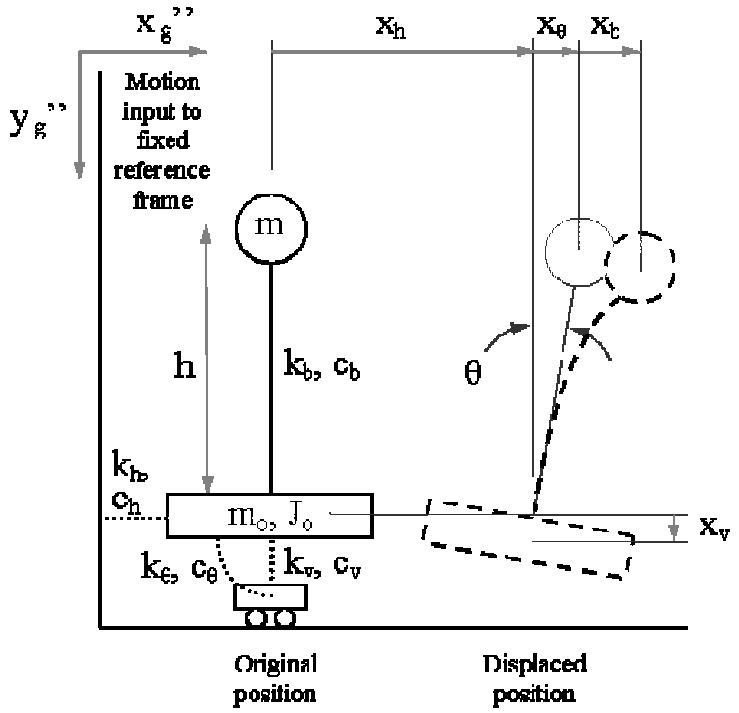

Figure 2: Four degree of freedom system.

3 MODEL DEVELOPLMENT AND EQUATIONS OF MOTION

The macro-element model described in this paper has been developed based on the existing macro-elements of Paolucci (1997), and Cremer et al (2001). The well-known general form of the equation of motion for a dynamic system is:

$$\boldsymbol{M}\ddot{\boldsymbol{x}} + \boldsymbol{C}\dot{\boldsymbol{x}} + \boldsymbol{K}\boldsymbol{x} = \boldsymbol{P} \tag{1}$$

where: $\boldsymbol{P}$ = input force vector, $\boldsymbol{K}$ = stiffness matrix, $\boldsymbol{C}$ = damping matrix, $\boldsymbol{M}$ = mass matrix, and $\boldsymbol{x}$, $\dot{\boldsymbol{x}}$, $\ddot{\boldsymbol{x}}$ = displacement, velocity, and acceleration vectors of the system respectively.

The macro-element is based around a four degree of freedom system, shown in Figure 2. The superstructure consists of a lumped mass with a single degree of freedom. The foundation has three degrees of freedom; rotational, horizontal, and vertical.

Because the behaviour of the soil is of the most interest at this stage of the macro-element development, the structural degree of freedom has been assumed to be linear. For simplicity, the damping of the system has been assumed to be constant. For the four degrees of freedom shown in Figure 2, the equations of motion can be obtained using the principles of dynamic equilibrium, or using Lagrange's equations. The resulting components of the general equation of motion (for linear elastic behaviour) for the model illustrated in Figure 2 are:

$$\boldsymbol{P} = \begin{Bmatrix} -m\ddot{x}_g \\ -(m+m_o)\ddot{x}_g \\ -mh\ddot{x}_g \\ -(m+m_o)\ddot{y}_g \end{Bmatrix} \qquad \boldsymbol{K} = \begin{bmatrix} k_b & 0 & 0 & 0 \\ 0 & k_h & 0 & 0 \\ 0 & 0 & k_\theta & 0 \\ 0 & 0 & 0 & k_v \end{bmatrix} \qquad \boldsymbol{C} = \begin{bmatrix} c_b & 0 & 0 & 0 \\ 0 & c_h & 0 & 0 \\ 0 & 0 & c_\theta & 0 \\ 0 & 0 & 0 & c_v \end{bmatrix} \qquad (2, 3, 4)$$

$$\boldsymbol{M} = \begin{bmatrix} m & m & mh & 0 \\ m & m+m_o & mh & 0 \\ mh & mh & m.h^2 + J_o & 0 \\ 0 & 0 & 0 & m+m_o \end{bmatrix} \qquad \boldsymbol{x} = \begin{Bmatrix} x_b \\ x_h \\ \theta \\ x_v \end{Bmatrix} \qquad (5, 6)$$

where:

- m = lumped mass of superstructure
- m_o = mass of foundation
- J_o = sum of second moments of inertia of the superstructure and foundation
- h = effective height of lumped mass above the centre of foundation
- $\ddot{x}_g$ and $\ddot{y}_g$ = horizontal and vertical input acceleration respectively
- k_b, k_θ, k_h, and k_v = structural, rotational, horizontal, and vertical stiffness coefficients for linear elastic behaviour respectively
- c_b, c_θ, c_h, and c_v = structural, rotational, horizontal, and vertical damping coefficients respectively

The macro-element has been coded using the MATLAB (MathWorks, 2005) software. The Newmark-beta numerical integration scheme has been adopted to solve the equations of motion, with which either the constant average, or linear, acceleration methods can be used. An incremental form of the equations of motion is used in the numerical integration procedure, as this is the most convenient method to undertake non-linear analysis. The error occurring as a result of the numerical integration method has been minimised through the use of Newton-Rhapson iterations with a second-order Runge Kutta method, and the use of transition steps where behaviour changes from elastic to plastic.

4 BEARING STRENGTH SURFACE AND PLASTICITY THEORY

The actions in the horizontal, rotational, and vertical degrees of freedom beneath the foundation are defined as H, M, and V respectively. These actions describe the reactions that the foundation imposes on the soil, rather than the equal and opposite reactions provided by the soil to the foundation, in accordance with the convention described by Butterfield et al (1997). The actions can collectively be described using one vector, F.

$$\boldsymbol{F} = \begin{Bmatrix} H \\ M \\ V \end{Bmatrix} \tag{7}$$

In routine analysis, soil is often assumed to behave in a linear elastic manner. This assumption is often reasonable, provided the soil is not approaching a state of failure. For shallow foundations, bearing failure occurs when the ultimate bearing strength of the soil beneath the foundation is mobilised, i.e. the soil cannot provide any additional reaction. When bearing failure occurs, the behaviour of the soil is strongly non-linear. If behaviour is assumed to remain linear elastic after bearing failure occurs, the calculated soil reactions will exceed those which can actually be provided to the foundation. Therefore, some way of accounting for the limitations of the bearing strength of the soil is required.

The most common way of calculating the ultimate bearing strength of soil beneath a shallow foundation is by using the well-known bearing strength equations. Alternatively, the combination of loads (moment, horizontal, and vertical) on a shallow foundation causing bearing failure can be represented by a three-dimensional surface in *H*, *M*, *V* space. This 'bearing strength surface' is a convenient method of defining bearing failure in the macro-element, as it is described by the three actions *H*, *M*, *V*, which are direct outputs from the model.

The bearing strength surface is described mathematically by a yield function, $f(\boldsymbol{F})$, where $f(\boldsymbol{F}) < 0$ when the actions locus is inside the bearing strength surface, and $f = 0$ when the actions locus is on the bearing strength surface. Note that $f(\boldsymbol{F})$ cannot exceed 0. A simple example of a yield function, and the one currently employed in the macro-element, is presented in Equation 8 (Nova and Montrasio, 1991). Figure 3 is a visual representation of the yield surface described by Equation 8, with V_{max} = 51,800 kN. It should be noted that any yield function can be programmed in the macro-element, enabling bearing strength surfaces corresponding to any sub-surface soil profile to be used.

$$f(F) = \left(\frac{H}{0.46 V_{max}}\right)^2 + \left(\frac{M}{0.5 a V_{max}}\right)^2 - \left(\frac{V}{V_{max}}\right)^2 \left(1 - \frac{V}{V_{max}}\right)^{1.9} \tag{8}$$

where a = width of foundation, and V_{max} = the static bearing strength under vertical load only. For a rectangular foundation V_{max} includes the contribution from shape and embedment depth factors.

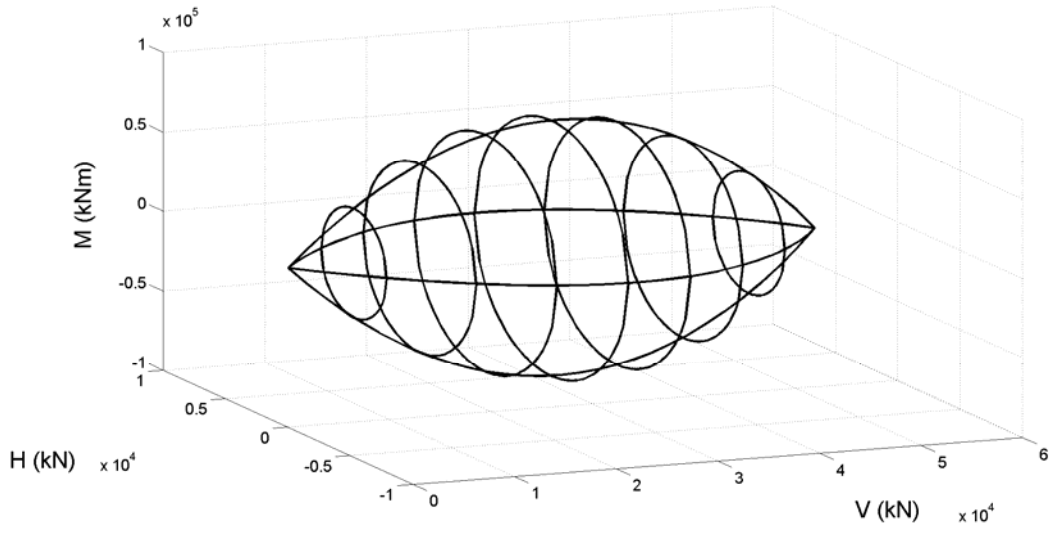

Figure 3: Bearing strength surface described by Equation 8 in three-dimensional *H*, *M*, *V* space.

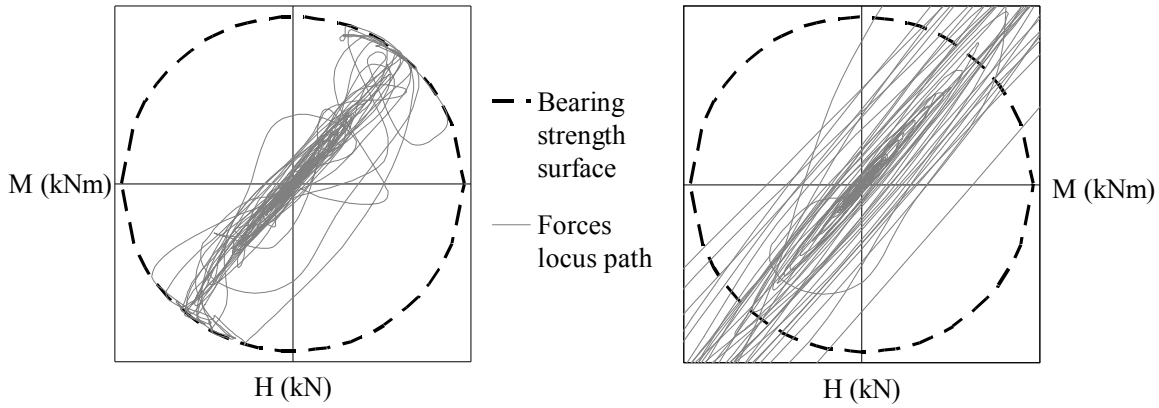

Figure 4: Perfectly plastic behaviour (left) compared with purely elastic behaviour (right).

In the macro-element, behaviour within the bearing strength surface is assumed to be linear elastic, and all displacements are fully recoverable. When the bearing strength surface is reached, behaviour is assumed to be perfectly plastic, that is, the bearing strength surface does not change in size or position. The actions locus (position of the actions in H, M, V space) cannot pass beyond the bearing strength surface, but can move around it.

Figure 4 illustrates how modelling with simple elastic behaviour for the foundation soil computes actions well beyond the bearing strength surface, and how the plastic part of the macro-element is able to contain the actions within or on the bearing strength surface. Other macro elements, for example those of Cremer et al (2001), Houlsby and Cassidy (2002), and Chatzigogos et al (2007b), use more complex plasticity models where the bearing strength surface changes in size and position based on the amount of accumulated permanent displacement (strain hardening), and irrecoverable displacements occur within the ultimate bearing strength surface.

Using the elastic-perfectly plastic model, permanent displacements occur when the forces locus is on the bearing strength surface (the soil is in a state of failure). In the macro-element, plastic behaviour is accounted for by modifying the stiffness matrix. All other components of the equations of motion remain the same. The stiffness matrix is modified according to the yield function, f, and the flow rule, g (discussed below). The formula used to calculate the elasto-plastic stiffness matrix is presented in Equation 9. The elasto-plastic stiffness matrix is no longer diagonal, resulting in the three foundation degrees of freedom becoming coupled. This means that rotation and horizontal movement of the foundation cause vertical displacement, even when there is no vertical input motion.

$$\boldsymbol{K}_{ep} = \boldsymbol{K}_e - \boldsymbol{K}_e \left(\frac{\delta \boldsymbol{g}}{\delta \boldsymbol{F}}\right)\left(\frac{\delta \boldsymbol{f}}{\delta \boldsymbol{F}}\right)^T \boldsymbol{K}_e \left[\left(\frac{\delta \boldsymbol{f}}{\delta \boldsymbol{F}}\right)^T \boldsymbol{K}_e \left(\frac{\delta \boldsymbol{g}}{\delta \boldsymbol{F}}\right)\right]^{-1} \tag{9}$$

where: $\boldsymbol{K}_e$ is the matrix of elastic stiffness components for the foundation.

The most important component in the calculation of the elasto-plastic stiffness matrix is the flow rule (or 'plastic potential'). The flow rule determines the direction and magnitude of plastic displacement. The flow rule is described by a mathematical function, $g(\boldsymbol{F})$. The value of $g(\boldsymbol{F})$ has no physical meaning; only the derivative of $g(\boldsymbol{F})$ is important. The derivative of g($\boldsymbol{F}$) defines the direction of plastic displacement vector, which is in a direction normal to $g(\boldsymbol{F})$.

Paolucci (1997) used a 'cornered ellipse' centred at $V/V_{max} = 0.5$, with a similar shape to the yield function, for his flow rule. This flow rule is specified in Equation 10. Paolucci's flow rule generates vertical displacements that are upwards (in the negative V direction) when $V/V_{max} < 0.5$, as can be seen from the left hand plot in Figure 5. This is considered to be unrealistic in the context of shallow foundations.

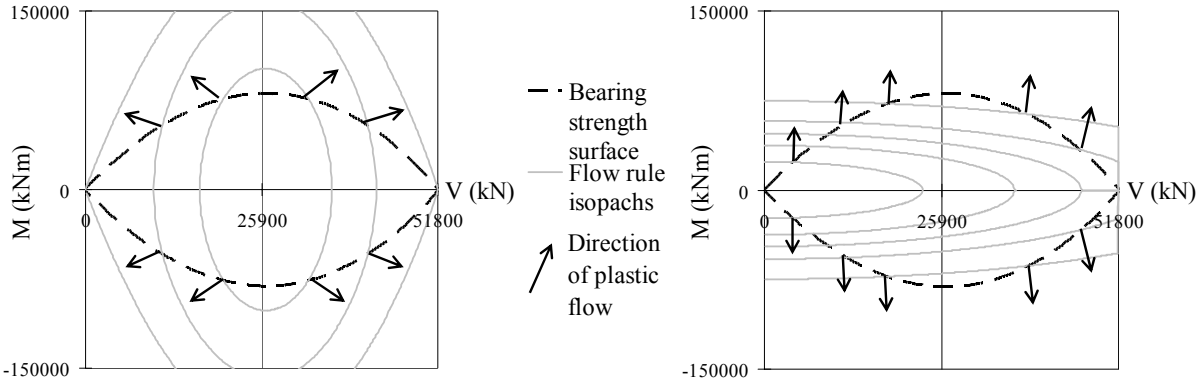

Figure 5: Two forms of flow rule, presented in *M*-*V* space. Left is a 'cornered ellipse' (Eq. 10), right is a 'centred ellipse' (Eq. 11). Overlaid is the bearing strength surface defined by Eq. 8, with V_{max} = 51,800 kN.

$$g(F) = 0.4^2\left(\frac{H}{0.46V_{max}}\right)^2 + 0.4^2\left(\frac{M}{0.5aV_{max}}\right)^2 - \left(\frac{V}{V_{max}}\right)^2\left(1-\frac{V}{V_{max}}\right)^{1.9} \tag{10}$$

$$g(F) = \left(\frac{H}{0.25V_{max}}\right)^2 + \left(\frac{M}{0.17aV_{max}}\right)^2 + \left(\frac{V}{V_{max}}\right)^2 \tag{11}$$

The flow rule adopted by Cremer et al (2001) is a smooth ellipse centred on the origin. This flow rule is specified in Equation 11. With this flow rule, plastic vertical displacements will always be downwards (in the positive *V* direction), although the magnitude of vertical displacement will be greater as *V* approaches V_{max}. This can be seen in the right hand plot in Figure 5.

5 MODELLING EXAMPLE

The system parameters adopted for this modelling example have mostly been adopted from Cremer et al (2002), and represent a bridge pier founded on a soil with a shear wave velocity of 130 m/s. This corresponds to an undrained shear strength of approximately 60 kPa, which in turn corresponds to a static vertical bearing capacity of roughly 360 kPa. The parameter values for the model are:

- m = 1500 tonnes, m_o = 500 tonnes, J_o = 22,100 tonnes/m^2, h = 15 m, a = 12 m
- V_{max} = 51,800 kN, FOS_{static} = 2.6
- $k_b = 6.3 \times 10^5$ kN/m, $k_h = 8.2 \times 10^5$ kN/m, $k_\theta = 1.7 \times 10^7$ kN.m/rad, $k_v = 1.0 \times 10^6$ kN/m
- $c_b = 4.3 \times 10^3$ kN.s/m, $c_h = 2.2 \times 10^4$ kN.s/m, $c_\theta = 1.2 \times 10^5$ kN.m.s/rad, $c_v = 3.4 \times 10^4$ kN.s/m

The system described above was subjected to the horizontal input acceleration from the 2005 Kobe earthquake (PGA = 8 ms^{-2}). The time step of the digital record used is 0.01 seconds. For clarity of results, no vertical input acceleration was used, although vertical input acceleration can be accommodated by the macro-element. The flow rule used was a smooth ellipse centred at the origin of *H*, *M*, *V* space, as described in Section 4 (Equation 11). Figures 6 to 8 present some output from the model.

Figure 6 presents plots of the input acceleration, and the total displacements of the lumped mass. Note how the vertical displacement (positive equals downwards) accumulates over time, as successive yielding of the soil beneath the foundation occurs. Since there is no vertical input motion, all vertical displacement is plastic, as a result of the coupling of the degrees of freedom during yielding. The total horizontal displacement of the mass is the combination of the foundation rotation and horizontal displacement, and the displacement of the lumped mass relative to the foundation ('structural distortion'). This total horizontal displacement is a combination of elastic and plastic displacements: note the residual total horizontal displacement at the end of the time history.

Figure 7 presents a plot of the path traced out by the foundation actions in *H*, *M*, *V* space, overlaid on the bearing strength surface. Note how the actions locus does not pass outside the bearing strength surface, but moves around it.

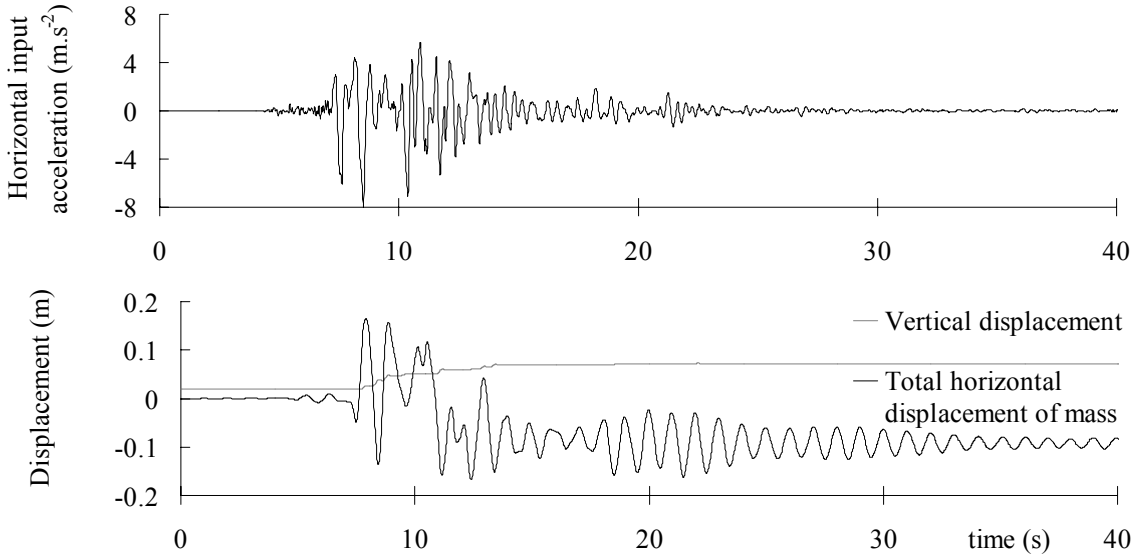

Figure 6:Input acceleration and total displacements versus time.

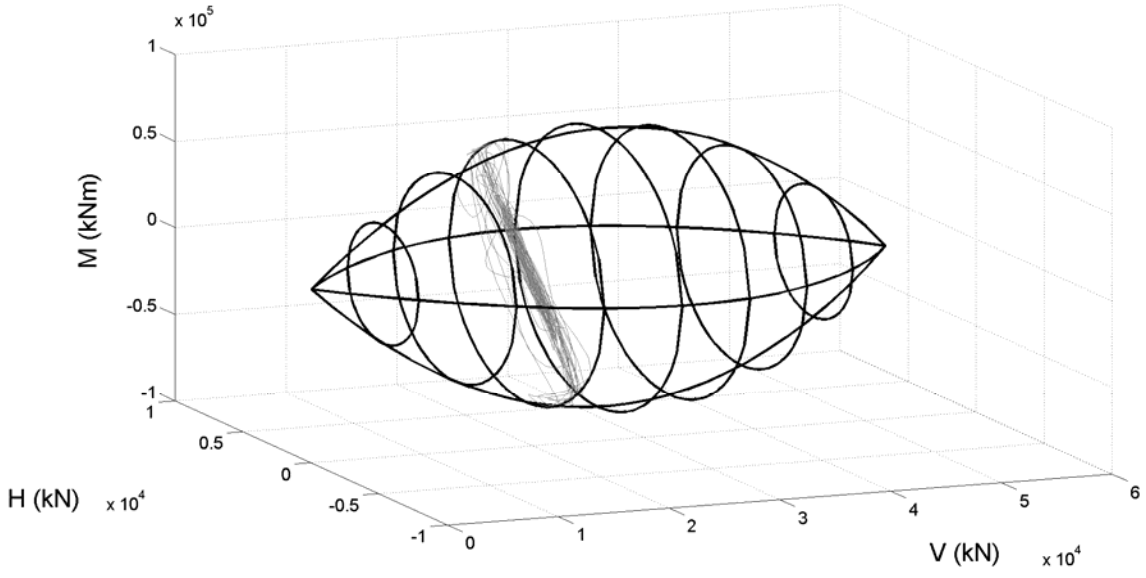

Figure 7: Force locus overlaid on bearing strength surface

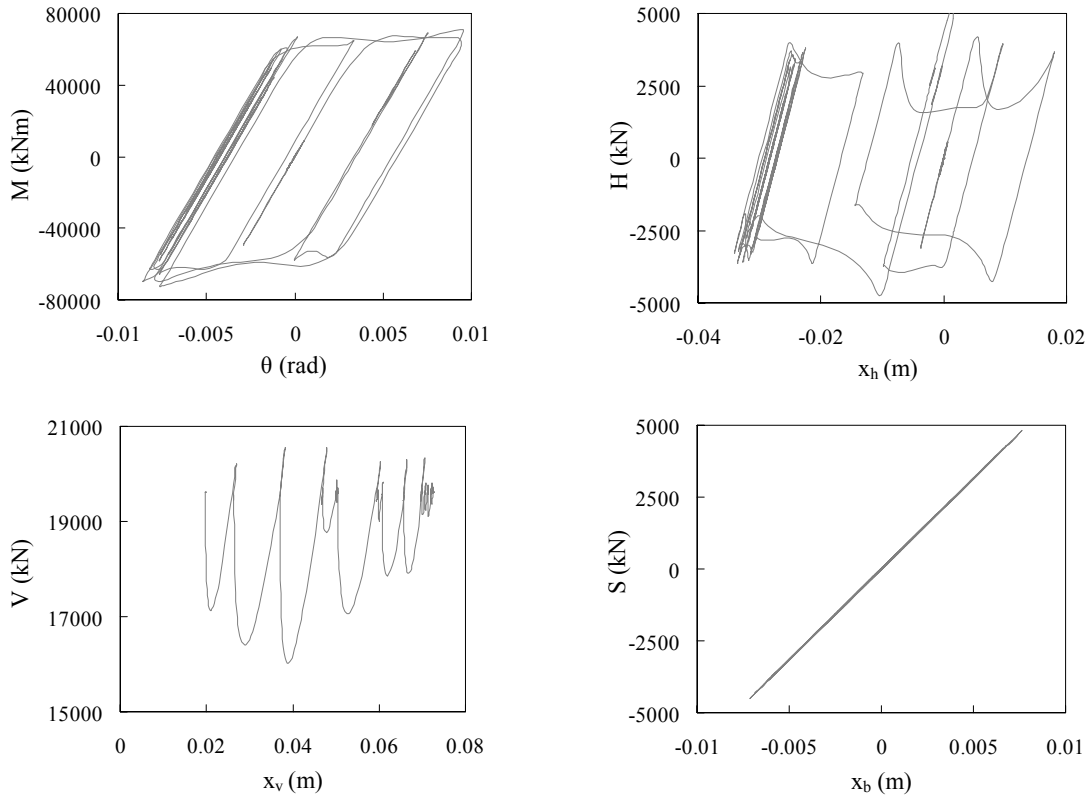

Figure 8: Forces versus displacements.

Figure 8 presents plots of actions versus displacements for all four degrees of freedom. Note how the M-θ and H-x_h plots are not what one would expect for one-dimensional perfect plasticity. This is because even though the actions locus cannot pass outside the yield surface, it can move around it. Hence H, M, and V can still increase or decrease during perfectly plastic deformation, provided the combination of all three forces remains on the bearing strength surface. The V-x_v plot shows the vertical force V 'jumping' as vertical displacement increases. This is due to the actions locus moving down and then back up the yield surface, as can be seen in Figure 7. This movement down and up the yield surface (in the V direction) is what allows the macro-element to predict vertical displacement upon yielding, even in the absence of vertical input motion.

6 **ADDITIONAL FEATURES**

Because of the way that the macro-element has been developed, it is relatively easy to include extra features. The practicality of these extra features may be limited, since they require additional input parameters, and make the macro-element slightly more complex to implement and understand. However, they allow the prediction of types of behaviour that have been observed to occur in shallow foundation systems.

6.1 *Stiffness degradation*

The linear elastic stiffness coefficients can be set to degrade as plastic rotation accumulates, as described by Paolucci et al (2007). This stiffness degradation model is based around the idea that plastic rotation causes a decrease in the contact area between the foundation and the soil, resulting in a reduced effective breadth. The elastic stiffness coefficients are decreased according to this reduced breadth. Figure 9 shows response spectra (calculated using the parameters and options in the Section 5 modelling example) with and without stiffness degradation. The period elongation due to the reduced stiffness is clear, as is the reduced total horizontal acceleration.

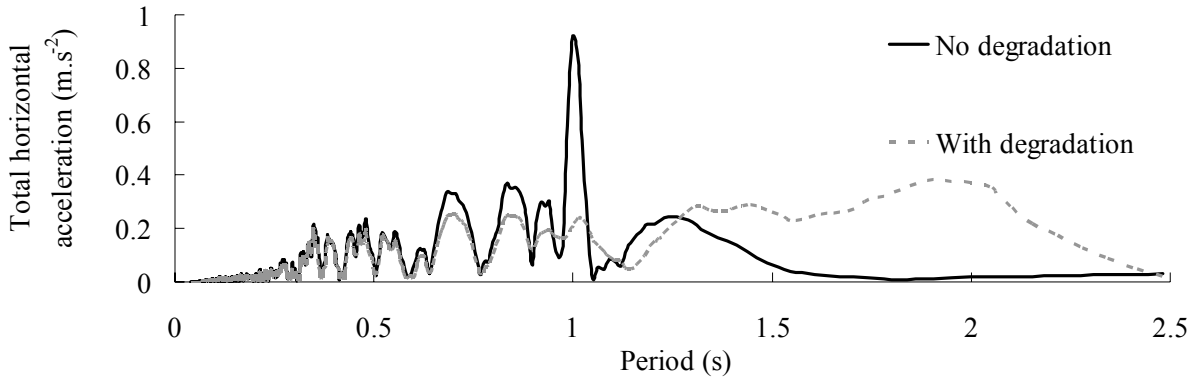

Figure 9: Response spectra with and without stiffness degradation.

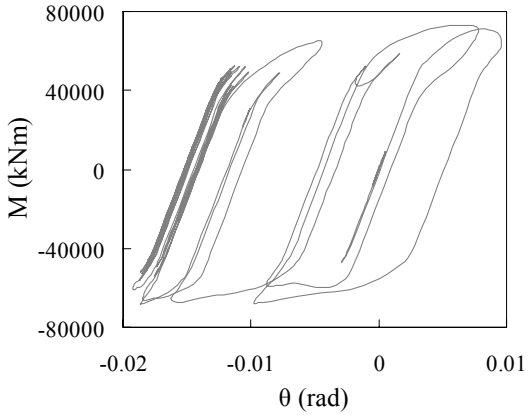

Figure 10: Moment-rotation diagram with uplift.

6.2 *Uplift*

The linear elastic stiffness coefficients can be modified if uplift is predicted to occur, as described by Chatzigogos et al (2007b). The occurrence of uplift is predicted based on the elastic rotation exceeding a calculated angle of uplift initiation. The inclusion of an uplift feature results in a lower rotational stiffness at higher angles of rotation, as shown in Figure 10. As a result, the moment-rotation diagram has more pronounced curvature as the system approaches yielding.

7 DISCUSSION AND OBSERVATIONS

7.1 *Type of flow rule*

The type of flow rule adopted has a major effect on the predicted vertical displacements. The flow rule adopted in the modelling example was a smooth ellipse, centred at the origin (shown on the right hand side of Figure 5). Figure 11 compares the results of the modelling example to an identical system with a flow rule in the shape of a cornered ellipse (shown on the left hand side of Figure 5). As described in Section 4, the smooth ellipse predicts downwards (positive) vertical movement, while the cornered ellipse predicts upwards (negative) vertical movement because $V \leq 0.5V_{max}$.

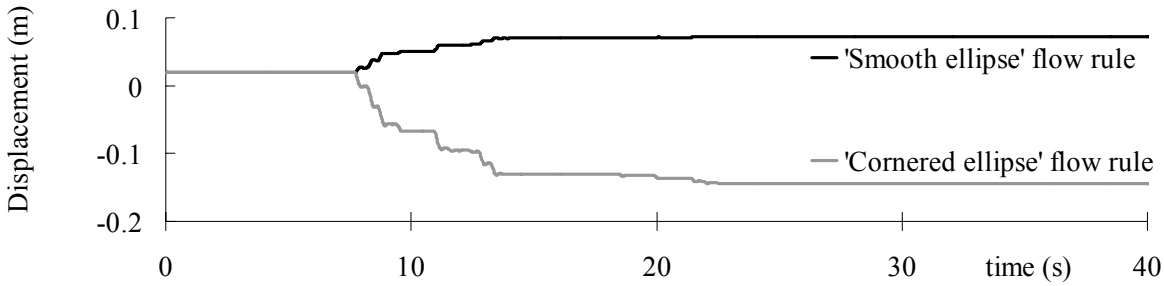

Figure 11: Vertical displacement versus time for two different flow rules.

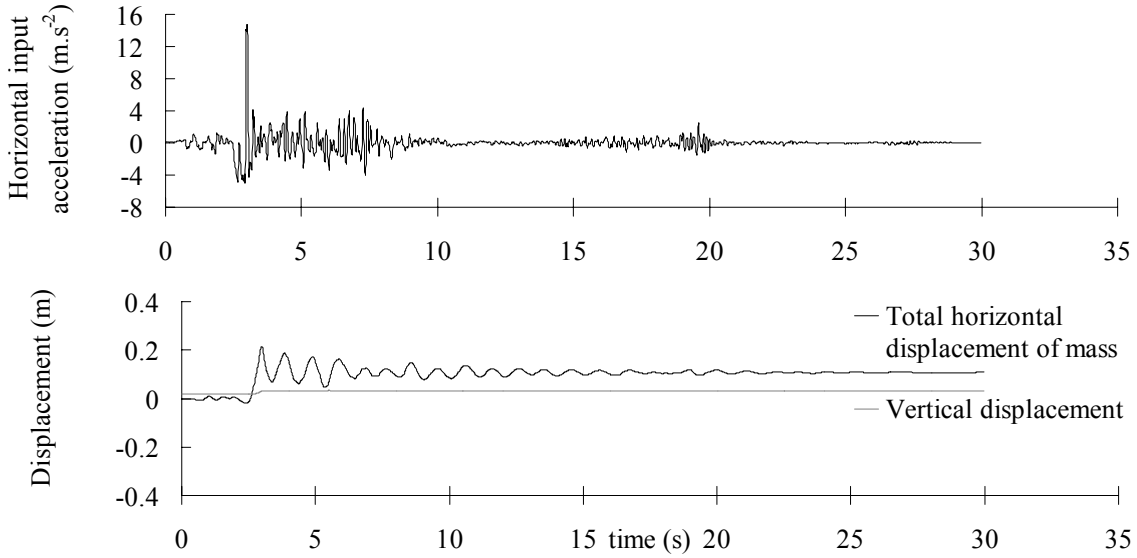

Figure 12: Input acceleration and total displacements versus time for a high magnitude, short duration, 'peaky' earthquake.

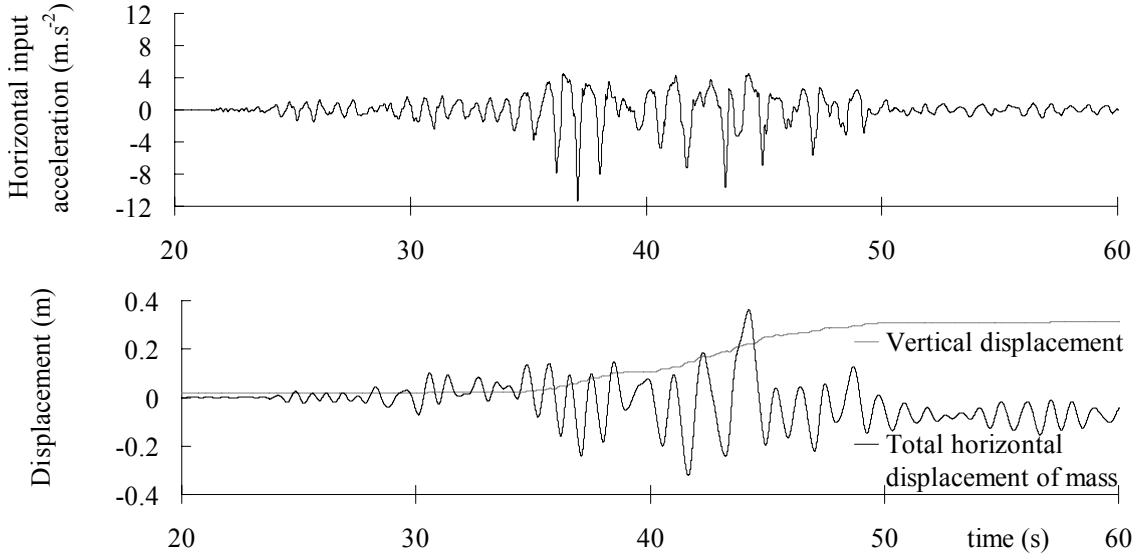

Figure 13: Input acceleration and total displacements versus time for a high magnitude, long duration earthquake.

7.2 *Accumulation of permanent displacements due to different input motion characteristics*

Because permanent vertical displacement only occurs when the yield surface is reached, the nature of the input acceleration has a significant effect on the accumulation of vertical displacement. The modelling example presented in Section 5 used a relatively long duration earthquake. Approximately 50 mm of permanent vertical displacement (settlement) was predicted to occur due to the prolonged and repeated yielding of the soil.

If the earthquake acceleration is of short duration, there will not be the same chance for vertical displacement to accumulate, even if the magnitude is higher. Figure 12 shows the total displacements that accumulate over time in response to one such 'peaky' earthquake (the 1992 Cape Mendocino earthquake, horizontal component only). The same system as used in the modelling example was used, and Figure 12 can be directly compared to Figure 6. The earthquake record used is characterised by a single, strong pulse, in one direction. As seen in Figure 12, this pulse is enough to cause the foundation to yield, leading to approximately 100mm of permanent rotational and horizontal displacement of the structural mass. However, because the foundation only yields momentarily, there is no chance for any significant settlement to accumulate. The total vertical displacement (settlement) at the end of the earthquake is predicted to be less than 20 mm.

If the earthquake acceleration is of long duration and high magnitude, there will be repeated yielding, resulting in significant accumulation of vertical displacement. Figure 13 shows the total displacements that accumulate over time in response to one such earthquake (the 1999 Chi-Chi earthquake, horizontal component only). The same system as used in the modelling example was used, and Figure 13 can be directly compared to Figures 6 and 12. The earthquake record is characterised by a long duration of high accelerations. This causes repeated and prolonged yielding beneath the foundation.

As seen in Figure 13, this yielding results in the accumulation of almost 300 mm of permanent settlement. The permanent total horizontal displacement is only about 100 mm, the same as for the short, 'peaky' earthquake shown in Figure 12. This is because plastic rotation and horizontal displacement occur in both directions, depending on the direction of input motion. Although there may be significant plastic rotation and horizontal displacement in both directions over the course of an earthquake record, the residual total horizontal displacement at the end of the earthquake may not be significant, as the movements in opposite directions end up cancelling each other out.

The results described above suggest that both the permanent vertical displacement and permanent total horizontal displacement (consisting of primarily of foundation rotation, but also of foundation translation and structural distortion) are strongly dependent on the nature of the input acceleration, but in different ways. The vertical displacement is dependent on the amount of yielding that occurs, so the longer duration of the earthquake, the more permanent settlement occurs. A high input acceleration does not necessarily lead to high settlement, if not much yielding occurs. The permanent total horizontal displacement is dependent on the individual characteristics of each earthquake. In many cases, there may not be any significant residual total horizontal displacement, especially if the earthquake has similar accelerations in both directions.

7.3 *Vertical factor of safety*

The system in the modelling example has a static FOS of approximately 2.6. This static FOS (V_{static}/V_{max}) can be changed simply by changing the value of V_{max}. A smaller value of V_{max} results in a lower static FOS, and also a smaller yield surface. A larger value of V_{max} results in a higher static FOS and also a larger yield surface. Figure 14 presents vertical displacement (settlement) and rotation versus time for three different static FOS: that used in the modelling example, and also FOS of half and double that used in the example (FOS of 1.3 and 5.2 respectively). The same earthquake record (1995 Kobe) was used for all three calculations.

In the modelling example (FOS = 2.6), residual settlement was predicted to be 50 mm. As discussed in Section 4, when there is a lower static FOS of 1.3 (that is, when V is closer to V_{max}), residual settlement is predicted to be significantly higher (approximately 180mm). When there is a higher static FOS of

5.2, residual settlement is predicted to be lower, but not significantly (approximately 30 mm). Mathematically, this is because the normal to the flow rule has a greater component in the positive V direction closer to V_{max} (see Figure 5, right hand side). This result is in accordance to what would intuitively be expected: the closer a foundation is to bearing failure before an earthquake, the more damage due to settlement is expected to occur to the foundation.

There is no link between the permanent rotation of the foundation and the static FOS. With FOS = 1.3, residual rotation is predicted to be positive 0.003 radians (clockwise). With FOS = 2.6, residual rotation is predicted to be negative 0.005 radians (anticlockwise). With FOS = 5.2, residual rotation is predicted to be negative 0.002 radians (anticlockwise). A lower FOS does not necessarily mean a higher residual rotation, and residual rotations are not even in the same direction. Instead, the residual rotation is mainly affected by incremental plastic rotations during the strongest phases of the input motion (occurring at approximately 10 seconds in Figure 14). A lower FOS will mean that the actions locus will remain on the bearing strength surface longer, but depending on the direction of motion, this may give a chance for the foundation to correct itself by rotating back towards its original position. The permanent horizontal displacements of the foundation have a similar, unpredictable behaviour.

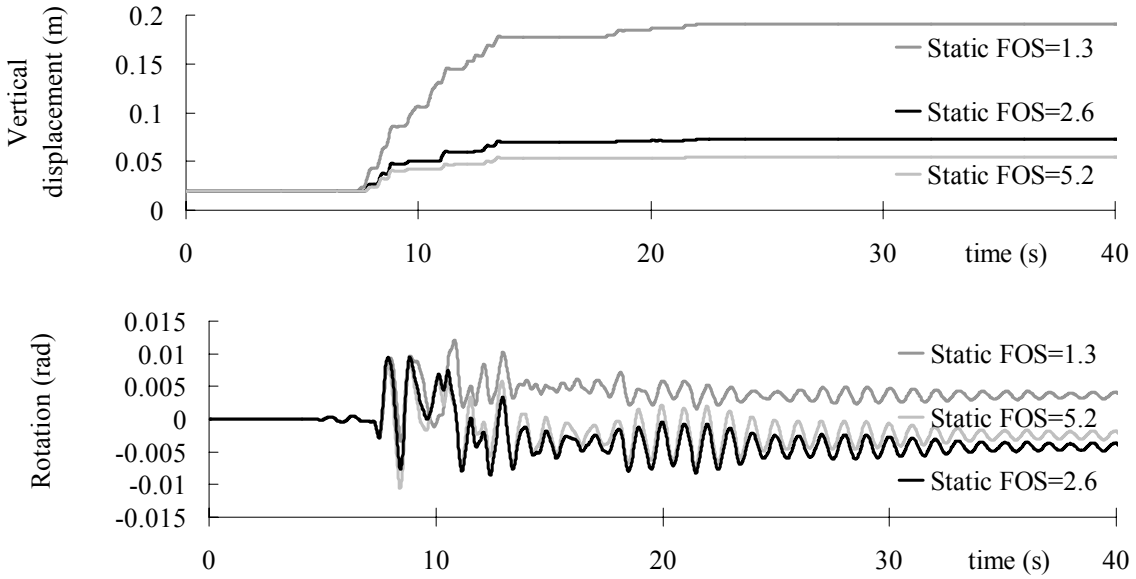

Figure 14: Vertical displacement and rotation versus time for various vertical factors of safety.

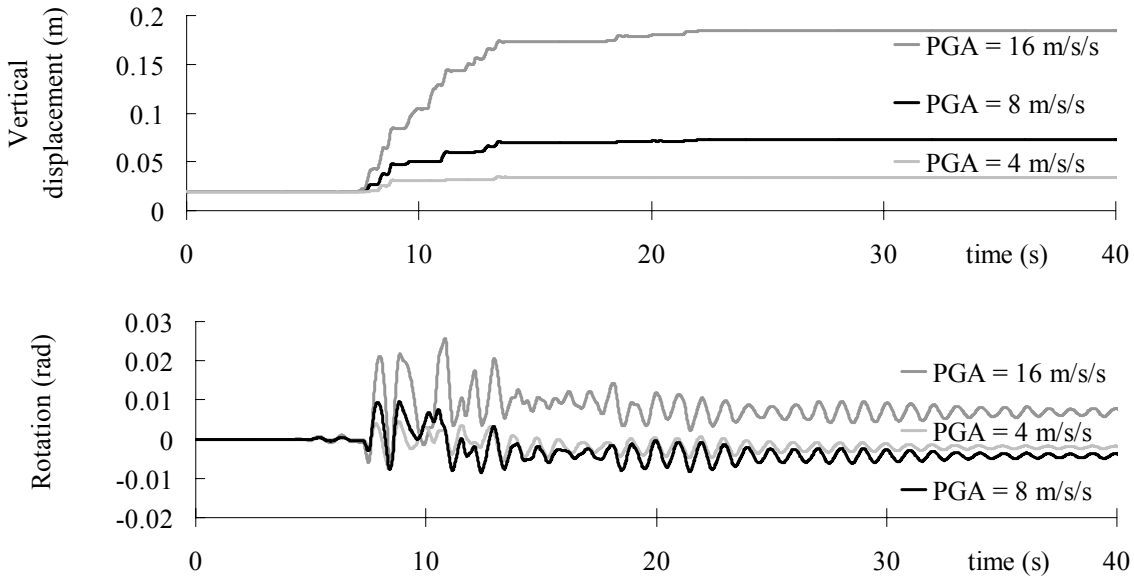

Figure 15: Vertical displacement and rotation versus time for various earthquake PGA.

7.4 *Earthquake PGA*

The modelling example in Section 5 used the horizontal component of the 2005 Kobe earthquake, with a PGA of 8 ms^{-2}. Figure 15 presents vertical displacement (settlement) and rotation versus time for three different PGA: the earthquake used in the modelling example, and the same earthquake record but with PGA scaled to half and double that used in the example (PGA of 4 ms^{-2} and 16 ms^{-2} respectively). For the purposes of this example, the entire earthquake record was scaled equally in order to achieve the desired PGA.

In the modelling example (PGA = 8 ms^{-2}), residual settlement was predicted to be 50 mm. With a higher PGA of 16 ms^{-2}, residual settlement is predicted to be significantly higher, at approximately 160mm. With a lower PGA of 4 ms^{-2}, residual settlement is predicted to be lower, at approximately 15mm. Even though the duration of the earthquake remains the same, a higher PGA means that more yielding occurs (the actions locus spends more time on the bearing strength surface). This results in higher residual settlements.

With regard to foundation rotation, the results are similar to those in Section 7.3 with varying static FOS. For the same reasons, no link can be made between the earthquake PGA and the residual rotation of the foundation: plastic rotation (and plastic horizontal displacement) of the foundation is dependent on the characteristics of the system combined with an individual earthquake record.

8 **PRACTICAL IMPLICATIONS**

Because of the way the macro-element has been developed, it should lend itself to implementation in routine structural analysis. The macro-element could be included as a separate foundation element with three degrees of freedom, and could be solved using common methods of numerical integration in the time domain. Earthquake records are commonly digitised using time intervals of either 0.02, 0.01, or 0.005 seconds. These time steps are usually adequate to ensure the stability of the macro-element. The macro-element can be adapted to suit any soil conditions, by way of modification of the soil stiffness and damping, yield function, and flow rule.

Many different types of structures can be modelled using the macro-element. At present, the type of structures that can be modelled are limited to those that can be represented by a lumped mass on a single ‘stalk’. These structures include bridge piers (in the transverse direction), storage towers, and multi-storey buildings having a uniform plan with height on a single pad or raft.

It is hoped to extend the capability of the macro-element to include multi footing structures, and single footing structures with more than one structural degree of freedom. Due to the additional complexity, this would probably best undertaken within an existing structural analysis program. This would also allow more complexity in the structural degrees of freedom, meaning both the foundation and structure could be allowed to yield during the earthquake. Then, the effects of the yielding beneath the foundation on the structural performance of the building can be assessed.

9 **CONCLUSIONS**

Macro-elements provide a simple but effective method of capturing the response of shallow foundation systems to dynamic loading. Because of their nature, no detailed information is obtainable on the stresses and strains of individual soil elements beneath the foundation; however all of the essential features of the foundation-soil interaction can be captured. These features include elastic behaviour at small displacements and plastic behaviour when bearing failure occurs.

The macro-element described in this paper enables simple four degree of freedom structure-foundation systems to be modelled. The macro-element predicts that the accumulated plastic settlement of the foundation is dependent on the magnitude and duration of the earthquake record, and the static FOS against bearing failure. The macro-element predicts that the accumulated plastic rotation and plastic horizontal displacement of the foundation is dependent on the characteristics of the system combined with an individual earthquake record. There is no direct link between either static FOS or earthquake

PGA, and plastic rotations and horizontal displacements.

We think this approach is particularly suitable for promoting integrated design of structure-foundation systems. Estimates of the permanent residual displacements of the foundation following an earthquake can be made. These provide an alternative method for design of shallow foundations, based on acceptable residual displacements as the criterion of satisfactory performance rather than bearing strength.

REFERENCES:

Butterfield, R., Houlsby, G.T., and Gottardi, G. 1997. Standardized sign conventions and notation for generally loaded foundations. *Géotechnique*, Vol. 47(5), 1051-1054.

CEN (Comité Européen de Normalisation). 2003. Eurocode 8, Part 5: Foundations retaining structures and geotechnical aspects. Draft 6, December 2003.

Chatzigogos, C.T., Pecker, A. & Salençon, J. 2007a. A macroelement for dynamic soil-structure interaction analyses of shallow foundations. *4th International Conference on Earthquake Geotechnical Engineering*. Paper No. 1387.

Chatzigogos, C.T., Pecker, A. & Salençon, J. 2007b. Macroelement modeling of shallow foundations. *Unpublished (personal communication)*.

Cremer, C., Pecker, A. & Davenne, L. 2001. Cyclic macro-element for soil-structure interaction: material and geometrical non-linearities. *International Journal for Numerical and Analytical Methods in Geomechanics*, Vol. 25, 1257-1284.

Cremer, C. & Pecker, A. 2002. Modelling of nonlinear dynamic behaviour of a shallow strip foundation with macro-element. *Journal of Earthquake Engineering*, Vol. 6(2), 175-211.

Gajan, S., Kutter, B., Phalen, J., Hutchinson, T., & Martin, G. 2005. Centrifuge modelling of load-deformation behaviour of rocking shallow foundations. *Soil Dynamics and Earthquake Engineering*, Vol. 25, 773-783.

Houlsby, G.T. & Cassidy, M.J. 2002. A plasticity model for the behaviour of footings on sand under combined loading. *Géotechnique*, Vol. 52(2), 117-129.

MathWorks, 2005. MATLAB v7.1 Student Edition.

Muir Wood, D. 2007. Modelling of Dynamic Soil Problems. In: *Earthquake Geotechnical Engineering*, Vol. 6 of: *Geotechnical, Geological, and Earthquake Engineering*, 131-149, Springer, The Netherlands.